NASA-TM-81634 19810006554

DOE/NASA/2593-20
NASA TM-81634

Deposition and Material Response from Mach 0.3 Burner Rig Combustion of SRC-II Fuels

G. J. Santoro, F. J. Kohl, C. A. Stearns,
G. C. Fryburg, and J. R. Johnston
National Aeronautics and Space Administration
Lewis Research Center

October 1980

Prepared for
U.S. DEPARTMENT OF ENERGY
Fossil Energy
Office of Coal Utilization

NOTICE

DOE/NASA/2593-20
NASA TM-81634

Deposition and Material Response from Mach 0.3 Burner Rig Combustion of SRC-II Fuels

G. J. Santoro, F. J. Kohl, C. A. Stearns,
G. C. Fryburg, and J. R. Johnston
National Aeronautics and Space Administration
Lewis Research Center
Cleveland, Ohio 44135

October 1980

Work performed for
U.S. DEPARTMENT OF ENERGY
Fossil Energy
Office of Coal Utilization
Washington, D.C. 20545
Under Interagency Agreement EF-77-A-01-2593

DEPOSITION AND MATERIAL RESPONSE FROM MACH 0.3 BURNER RIG COMBUSTION OF SRC-II FUELS

by G. J. Santoro, F. J. Kohl, C. A. Stearns, G. C. Fryburg, and J. R. Johnston

National Aeronautics and Space Administration
Lewis Research Center
Cleveland, Ohio 44135

E-647

ABSTRACT

Collectors at 1173K (900°C) were exposed to the combustion products of a Mach 0.3 burner rig fueled with various SRC-II fuels (i.e., industrial turbine liquid fuels from solvent refined coals). Four fuels were employed - a naphtha, a light oil, a wash solvent and a mid:heavy distillate blend. The response of four superalloys (IN-100, U-700, IN-792, and Mar M-509) to exposure to the combustion gases from the SRC-II naphtha and resultant deposits was also determined. The SRC-II fuel analysis and insights obtained during the combustion experience are discussed. Particular problems encountered were fuel instability and reactions of the fuel with hardware components.

The major metallic elements which contributed to the deposits were copper, iron, chromium, calcium, aluminum, nickel, silicon, titanium, zinc, and sodium. The deposits were found to be mainly metal oxides. An equilibrium thermodynamic analysis was employed to predict the chemical composition of the deposits. The agreement between the predicted and observed compounds was excellent. No hot corrosion was observed. This was expected because the deposits contained very little sodium or potassium and consisted mainly of the unreactive oxides. However, the amounts of deposits formed indicated that fouling is a potential problem with the use of these fuels.

INTRODUCTION

Over the past 20 years, it has been demonstrated that liquid fuels can be derived from coal by a number of processes. One of these is known as the Solvent Refined Coal Process (SRC) (Ref. 1). There are ambitious national programs underway to manufacture and use coal-derived liquid fuels in this country by the end of the decade. Based on promising laboratory and pilot plant results, it appears that large commercial-scale SRC units could be in operation in the late 1980's and the 1990's. In the meantime, potential problems associated with the use of such new fuels must be analyzed and resolved before their commercial implementation. The areas under study include the manufacturing parameters and economics, storage stability and handling, safety and pollution aspects, and compatibility with the type of machinery in which the fuel may be used.

Coal is not burned directly in gas turbines because of both accelerated erosion and of the troublesome deposits that can arise due to the high ash content. Even though a substantial portion of the metallic elements are removed from coal-derived liquids (Ref. 2), both solid (SRC-I) and liquid (SRC-II) fuels derived from coal are expected to contain some metallic element impurities. This may lead to the formation of inorganic ashes and/or highly corrosive salts in practical combustion systems. Once condensed, these compounds can corrode, erode, or foul surfaces exposed to combustion products. For example, "hot corrosion" is associated with the condensation of sodium sulfate on gas turbine blades (Ref. 3) when sulfur and sodium are present in the fuel/air mixture. Additionally, corrosion from reactive gaseous species, such as alkali halide vapors, is a possibility (Ref. 4). The presence of iron, calcium, and phosphorus can lead to deposits which can cause severe turbine-blade cooling-hole plugging (Ref. 5). It is also well known

that ash particles can cause severe erosion of surfaces (e.g., Ref. 6). From current knowledge, one could expect that hot corrosion of the type encountered in aircraft, marine or industrial-type gas turbine engines may also be a major problem for machines utilizing coal-derived fuels, because the chemical elements responsible for the corrosion are naturally occurring impurities in the coal. Moreover, some of these impurities will not be completely removed from the fuels by proposed processing techniques.

One of the objectives of the Gas-Turbine Critical Research and Advanced Technology Support Project (Ref. 7), sponsored by the Dept. of Energy at the Lewis Research Center, is to obtain a basic understanding of the behavior of inorganic impurities in fuels with respect to deposition, corrosion, and fouling. Significant progress has already been achieved in some aspects of this effort (Refs. 8,9, and 10). Other recent DOE- and EPRI-sponsored research programs have been carried out to evaluate the effects of combustion products on gas turbine hot-section components and to monitor a number of combustion parameters. The first of these studies (Ref. 11) used mainly synthetically-doped fuel oils while the second (Ref. 12) employed actual coal-derived liquids.

The objective of this investigation was to characterize experimentally the deposition phenomenon and resultant material response (corrosion and erosion) of typical superalloys in a Mach 0.3 burner rig. Deposition tests were run with four SRC-II fuels (designated as naphtha, light oil, wash solvent, and mid:heavy distillate blend). The formation and chemical composition of the expected deposits were predicted from the predetermined impurity contents of the fuels by use of a computer program which employed equilibrium thermodynamics to describe the complex distribution of chemical species in the combustion products. The response of four superalloys (IN-100, U-700, IN-792

and Mar M-509) from exposure to combustion products and the actual deposits which formed was established for the SRC-II naphtha fuel. Only deposit formation was studied for the light oil, wash solvent, and mid:heavy distillate blend.

EXPERIMENTAL PROCEDURES

Two types of burner rig experiments were performed: 1) deposition and 2) corrosion. In the deposition tests, the combustion gases were directed toward either a carrousel with 8 superalloy specimens (for the naphtha fuel) or an inert collector (for the light oil, wash solvent, or mid:heavy distillate blend fuels). The material deposited from the combustion gases was analyzed and the results were compared with those predicted from thermodynamic considerations. In the corrosion test, four different superalloys were exposed via the carrousel to the combustion gases produced by burning the naphtha. Thus the naphtha fuel, which was available in the largest quantity and was burned first, was used in a combined deposition/corrosion test. The corrosion resistance of the alloys was followed by periodically weighing the alloy specimens and was later confirmed by metallographic examination. The procedural details and results of these tests are given in sections below.

Fuel Characterization - All of the four SRC-II fuels used (naphtha, light oil, wash solvent, and mid:heavy distillate blend) were obtained from the Pittsburgh and Midway Coal Mining Co. (P and M) of Dupont, Washington, a subsidiary of Gulf Oil Corp. The chemical analyses and other properties of the fuels are given in Table I.

The analyses for the major elements (C, H, O, N, S) were carried out by the Gulf Research and Development Co. for the naphtha, light oil, and wash solvent and by P and M for the mid:heavy distillate blend. Sulfur analyses

were performed also at the Lewis Research Center. The heat of combustion determinations and organic molecular type analyses were performed by Gulf Research and Development Co. or P and M. The complicated organic compositions of these fuels are similar to that of other coal-derived liquids (Ref. 13). In-house determination of the trace elements consisted of a dry ashing procedure, followed by spectrographic analysis using an argon-stabilized d.c. arc technique (Ref. 14), developed at Lewis Research Center, and corroborated by atomic absorption spectrometry.

The analysis of liquid hydrocarbons for trace metals can in many instances lead to results with a high level of uncertainty. The accuracy of the in-house analyses for trace elements was estimated to be $\pm$ 50 percent of the amount reported. The limits on accuracy were established using the method of successive dilutions (first employed by Gilbert (Ref. 15)), simulation of calibration standards, and comparison of the emission spectrographic and atomic absorption results. The significance and consequences of the trace element constituents of the various fuels will be discussed in subsequent sections.

The SRC-II naphtha is a light distillate product from the P and M Fort Lewis, Washington pilot plant. It contains benzene, toluene, xylene, phenols, and higher homologs. It also contains hydrogen sulfide and mercaptans. Because of this, the fuel was very odorifurous and possibly toxic. Thus, several safety and health hazards were associated with this fuel and appropriate measures had to be taken with respect to its storage and handling.

The mid:heavy distillate blend fuel was designated by P and M to be a 2.9 Middle Distillate to 1 Heavy Distillate fuel oil made in the SRC-II mode of operation by using Powhatan No. 5 mine coal.

Burner Rig - All of the SRC-II fuels were combusted in a Mach 0.3 burner rig operated at a combustion gas pressure of $6.9 \times 10^3 N/m^2$ (1 psig). The rig was patterned after those used in the past at NASA Lewis Research Center (Ref. 16). The burner (see figure 1) consisted of a housing, about 28 cm long by about 7 cm in diameter, with an exit nozzle attached at one end and with a backplate attached to the other end. A burner can or liner was contained within the housing. The exit nozzle was made of the cobalt-base superalloy L605 and had a throat diameter of 2.5 cm. The backplate contained the fuel nozzle and had the combustion air and fuel lines attached to it. The burner liner was fitted with a swirl plate with a tapered hole in its center, about 1.5 cm diameter at its outer surface down to about 1 cm diameter, to accomodate the fuel nozzle. Around the center hole in the swirl plate were 10 concentric large primary air holes and around these were 10 smaller primary air holes. All the air holes were angularly drilled to give a swirling motion to the combustion air for better mixing with the fuel. Secondary air passes around the swirl plate and liner and enters the combustion zone through hole in the liner. Fitted perpendicularly through the housing and the liner, about 3.8 cm downstream of the fuel nozzle, was a spark ignitor to initiate combustion. In the final version of the rig the combustion was self-sustaining after ignition as long as fuel and air were continuously supplied in the proper ratio. The burner was capable of consuming up to 7.6 liters (2 gals) of fuel per hour and 140 kg (300 lbs) of air per hour.

In the deposition and corrosion tests, either a carrousel that would accomodate eight wedge-shaped superalloy specimens or a single collector was located downstream of the burner exit nozzle. The carrousel or collector was rotated between 300 and 500 rpm about an axis prependicular to the flame. The burner was pivoted in and out by a pneumatic operator so that either the

burner combustion gases or the blast from an air supply was directed at the specimen/collector. The cooling air was used to force-cool the specimens during the cooling cycle.

Test Site and Safety - The burner rig and its control console were designed to be moveable. (They were constructed at the Lewis Research Center and shipped to the NASA-Plum Brook Station in Sandusky, Ohio, where the burner runs were conducted). Thus all of the burner rig components were mounted on a 0.6 x 1.5 meters test stand 1.0 meter high. Cables and tubing were connected from the test stand in the test cell to a single control console in the control room. Fuel and air lines from sources outside the test cell were hooked up to the test stand.

The burner rig was designed to operate unattended. Provisions for unattended operation consisted of a closed loop system to control the specimen temperature; automatic shut down if permissive limits were violated (e.g., air or fuel pressures); timers to actuate heating and cooling cycles and to shut the burner off after the completion of a predetermined number of cycles; and automatic shut downs for emergency purposes such as flame out, fire in the cell, specimen overtemperature, or lack of specimen rotation. Figure 2 is an air and fuel supply schematic.

Because of the toxicity of the as-received fuel (mentioned above), the tests were conducted at an isolated site at the NASA Plum Brook Station. The control console was in an adjacent room separated from the burner rig cell by a concrete wall equipped with an observation window. The air was supplied by a compressor located at another part of the station while the fuel sources were located out-of-doors in a depression (to contain potential spills) about 45 meters (150 feet) from the test cell. The naphtha fuel was contained in a 19 m^3 (5000 gal) capacity fuel trailer while the other fuels were contained

in 208 liter (55 gal) drums. A low pressure pump circulated the naphtha in the trailer to maintain uniformity of the fuel. This pump also provided the head for the high pressure pump, 2.1×10^6 N/m^2 (300 psig) output pressure, which fed the fuel to the test cell through 0.95 cm (3/8 inch) stainless steel tubing. When operating from the drums, the head for the high pressure pump was provided by gravity. The high pressure pump was activated from the control room and was turned off as part of the automatic shutdown system. Figures 3a and 3b are photographs of the fuel supply area showing the trailer and fuel pumps. The photographs were taken during the deposition/corrosion test with naphtha; thus no fuel drums are shown.

Burner Rig Experience with SRC-II Fuels - It was anticipated that some modifications in burner rig hardware or operating procedures might become necessary for combustion with the SRC-II fuels. As expected, the burner rig functioned flawlessly with Jet A-1 fuel pumped from a drum during preliminary testing. However, within minutes of the beginning of burning with naphtha, the burner flamed out. The naphtha, which originally had a pinkish color when received in the spring of the year, had turned amber by August and by test time in September was brown-black. An analysis showed the dark color of the fuel was accompanied by the precipitation of elemental sulfur needles. The sulfur was identified by X-ray diffraction. No other phases were detected. The complete analysis of the precipitate is given in Table II. These needles, which were visible under 10X magnification, had clogged the fifty micron size fuel filters and the fuel nozzle screen. At this time an analysis of the vapors above the fuel in the trailer revealed that the H_2S level had decreased to only a trace amount, i.e., a few parts per million. Originally, P and M had measured H_2S levels as high as 42,000 ppm above the naphtha fuel in the original tank car and 16,000 ppm on the outside of the tank car. This

level decreased considerably during the time of shipment and storage. A value of 1000 ppm was measured outside of the storage trailer after several months of storage at the Plum Brook Station. Apparently much of the sulfur originally present as H_2S had been oxidized to elemental sulfur. To rid the fuel of the precipitate, an 80 gallon per minute (303 l min^{-1}) bag-type pressurized industrial filter was installed in the fuel line close to the trailer; see figure 3.

Subsequently, the burner functioned for 14 one hour cycles before flaming out due to coking of the burner liner. An analysis of the metal content of the coke is given in Table II. Only a 1.3 cm diameter free passage remained in the 5.0 cm I.D. liner. To reduce the rate of coking and thus extend the intervals between servicing the rig, a combustion air preheater was installed. The air preheater had a maximum temperature capability of less than 260°C (500°F). This modification increased the number of cycles to 30 before coking again caused a flame out. To further decrease the coking, a higher temperature preheater was installed with a maximum air temperature of close to 430°C (800°F). With the combustion air preheated to this temperature the fuel nozzle became hot enough to decompose the fuel in the nozzle causing it to clog and the burner to flame out within two minutes of ignition. To cool the nozzle, the fuel flow was increased from about 7.6 liters (2 gals) per hour to 190 liters (50 gals) per hour through a modified backplate designed so that most of the fuel bypassed the nozzle and returned to the trailer. Thus the nozzle was cooled by the fuel. After this last modification no coking occurred. However, during the late-fall season the ambient temperature began to drop to 4°C (40°F) and a tar-like substance formed on the liner and holes of the swirl plate. Eventually the ambient temperature dropped to -1°C (30°F); it then became difficult to get the burner

to run for even one or two cycles. At this juncture the superalloy specimens had been exposed for a sum total of 191 cycles and it was decided to terminate the corrosion test for lack for any evidence of accelerated oxidation due to the impurities in the fuel. Weight change data and visual examination which was taken when the experiment was interrupted indicated a deposit was forming on the specimens but little corrosion was occurring.

Numerous leaks occurred in the fuel lines during this study for which tightening the connections only temporarily stopped. It was subsequently discovered that the fuel was corroding the copper conical seals in the A and N fittings. The seals were removed and the stainless steel lines were coupled without any seals and the leaks ceased. Samples of the fuel had been taken at the 0th, 120th and the 191st cycles and analyzed for various metallic elements and for sulfur and chlorine. The results of these analyses are give in Table III. It is apparent that the amounts of copper, iron, nickel, and zinc, along with sulfur and chlorine, had increased significantly over the time period when the fuel had been used. Presumably, the increase of the metal content was caused by corrosion of the fuel system fittings and tankage components by ingredients in the fuel. At the time of the 191st cycle point the SRC-II naphtha has been stored in the original shipping tank car and storage trailer for about 11 months.

Deposition/Corrosion Test Procedure with Superalloy Specimens - Eight wedge-shaped specimens of the dimensions shown in figure 4 were mounted in a carrousel specimen holder, figure 5. Two specimens were U-700, two were IN-792, two were Mar M-509, and one was IN-100. Mar M-509 is a cobalt-base superalloy, the others are nickel-base superalloys. The nominal composition of these alloys is given in Table IV. The selection of alloys for this test was made on the basis of their relative corrosion resistance (Ref. 10): IN-100

has poor corrosion resistance, MarM-509 has excellent resistance and U-700 and IN-792 have intermediate resistances. The eighth position of the specimen holder was occupied by a dummy specimen, a FeCrAlY alloy, with the same geometry as the test specimens. The dummy specimen had a hole through its long axis from the bottom to within 2.54 cm of its top; a thermocouple inserted into the hole had its junction positioned at what was to be the hottest zone of the specimen (pyrometer determined) when exposed to the burner flame. The leads of the thermocouple were extended through a hole in the bottom of the holder and into the hollow shaft supporting the holder. The leads were further extended through another hole further down the shaft to a temperature compensator and then to a slip ring assembly attached around the shaft. This assembly allowed temperature measurements to be made on the rotating specimen. The output of the slip ring was transmitted to the control room. The temperature of the specimens was also monitored by an optical pyrometer sighted from the control room through the observation window.

The fuel-to-air ratio was automatically adjusted to provide a hottest zone constant temperature on the specimens of 1173K (900°C). The temperature reading used for this adjustment was sensed by a visible radiation pyrometer attached to the rig. The signal from this pyrometer was fed to a controller which operated an electric-to-pneumatic transducer which in turn adjusted the fuel valve. Because combustion air pressure was set manually, control of the fuel valve controlled the fuel-to-air ratio and thus the temperature. The experiment was run in a cycling mode which consisted of one hour at temperature and three minutes of forced air cooling.

The exposed specimens with their deposits were analyzed by X-ray diffraction. The maximum depth of the corrosion attack was determined metallographically as follows. Prior to the burner rig exposures the original

thickness of each specimen was measured along the diameter at the "plane of sectioning" (figure 4) with a bench micrometer caliper. At the completion of the burner exposure each specimen was sectioned at the plane of the original thickness measurements. The cross-sections were metallographically prepared and then examined under a cathetometer-type microscope at a 100X magnification and the thickness of the alloy specimen visibly unaffected by the corrosion attack was measured. Total affected alloy thickness included the thicknesses of scales, internal corrosion, locally corroded grain boundaries, plus zones depleted in any of the alloy's original elements (seen visibly by the absence of a second phase, e.g., $\gamma'[Ni_3(Al,Ti)]$ phase in a γ-γ' alloy, where the gamma is Ni solid solution). The difference in the original metal thickness and the unaffected alloy thickness divided by two was defined as the maximum depth of attack. The rationale for use of this procedure was that for engineering purposes only that thickness of alloy not so affected can be considered mechanically sound. Of course, the accuracy of these measurements varies depending on the morphology of the attack. A uniform broad front attack with sharp interfaces would permit an accuracy of about $\pm$ 10 μm in the maximum depth of attack value. However, such attack seldom occurs. Undulating interfaces, internal corrosion, and grain boundary penetration are more common. If not too severe, a value accurate to about $\pm$ 30 μm is possible in this more general situation, but it can be as large as $\pm$ 50 μm.

Deposition Test Procedure with Inert Collector - A schematic diagram of the collector and its holder is shown in figure 6. The collector was a platinum-10 weight percent rhodium (Pt-10Rh) slightly tapered hollow cylinder about 1.3 cm long (.5 inches) and 1.3 cm in diameter and about 0.13 mm (5 mils) thick. The small size of the collector was chosen to facilitate temperature uniformity over the entire surface when exposed to the burner

flame. The collector was mounted snugly over a hollow support made of IN-600. The junction of a thermocouple was peened into a hole in the wall of the collector support. The thermocouple leads extended through the support, the stem and out the base, and were attached to contacts on the slip ring assembly referred to previously. The collector was maintained at a temperature of 1173K (900°C) for the duration of the deposition tests. Duplicate isothermal tests were run with the wash solvent and light oil cuts of the SRC-II fuels. The burner rig configuration was identical to that used in the deposition/corrosion test with the naphtha fuel. The runs were terminated after several hours because sufficient deposit for analysis was accumulated in that time. These runs were continuous, not cyclic.

For the deposition tests with the mid:heavy distillate blend fuel, duplicate isothermal runs of about one hour were made, but the configuration of the burner had been drastically changed from that used in the two previous deposition tests. Prior to the runs with the blend fuel the burner had been modified to burn a mixture of 60 percent No. 2 distillate fuel oil and 40 percent coal dust. The details of this test will be reported elsewhere (Ref. 17). The coal-oil burner configuration was also used for the mid:heavy distillate blend fuel deposition runs. The main feature of this configuration was the use of a sonic fuel nozzle wherein the fuel and some of the air was premixed before entering the burner. This premixing of the fuel and air reduced the range of fuel-to-air ratios that would sustain combustion; under the lowest usable fuel-to-air ratio the collector's temperature could not be kept down at 1173K (900°C). To attain the desired collector temperature it was necessary to move the collector (along with entire rotation assembly) further away from the exit nozzle. The previous distance from the exit nozzle

to the surface of the collector of 5 cm (2 inches) was increased to 24 cm (9.5 inches) for the test with the blend fuel.

The deposits from all of the deposition tests were examined optically and by SEM, X-ray diffraction, emission spectroscopy, and X-ray spectral analysis.

THERMODYNAMIC ANALYSIS AND PREDICTION OF DEPOSIT COMPOSITION

The objective of the theoretical analysis was to calculate the composition of gaseous and condensed phase products of SRC-II fuel/air combustion by taking into account the trace metal content of the fuel. Previous studies (Refs. 18, 19 and 20) have indicated that the condensed phases predicted by a thermodynamic analysis are the ones likely to appear as deposits. Toward this end, the widely used NASA Lewis Complex Chemical Equilibrium Computer Program (CEC) (Ref. 21) was employed to calculate adiabatic flame temperatures, compositions of combustion gas at any temperature, composition of condensed pure phases (if any form), and thermodynamic dew points for condensation. References 18, 19 and 20 give pertinent examples of these sorts of applications. The CEC program is based on the minimization of free energy approach to chemical equilibrium calculations subject to the constraint of maintaining a proper mass balance between reactants and products. The program permits the calculation of chemical equilibrium composition for homogeneous or heterogeneous systems for assigned thermodynamic states such as temperature-pressure (T,P) and enthalpy-pressure (H,P). For the present work, the role of the trace elements in the SRC-II fuels was examined in terms of compositions of the gaseous and condensed (solid or liquid) phases as a function of temperature.

The input parameters for use with the CEC program are listed in Table V. The trace elements were chosen to be considered in the thermodynamic analysis

on the basis of several criteria: 1) that the element was present in the fuel at a level of 0.1 wppm or greater; and 2) that sufficient thermodynamic data were judged to be available for gaseous and condensed phase compounds of the element. Even when these somewhat restrictive criteria were applied, no "major" trace elements were omitted from consideration. The only possible exceptions to this were the elements manganese (Mn) (present in the light oil, wash solvent, and mid:heavy distillate blend) and tin (Sn) (present in the naphtha) where the thermodynamic data base was judged to be insufficient. The gaseous and condensed phase compounds considered by the program are listed in Tables VI and VII. Most of the thermodynamic data were obtained from the JANAF tables (Ref. 22) or the compliation of Barin and Knacke (Ref. 23). Data for several compounds were generated in-house.

Calculations were performed to simulate the actual conditions of combustion for the SRC-II fuels run in the burner rig deposition and corrosion tests. The computer program was operated in the H,P mode with the initial and final enthalpies equal to that of the reactants at the inlet temperatures in order to calculate the equilibrium adiabatic flame temperatures. These results are given in Table VIII along with the chemical composition of the products. The trace species molecules listed are the ones which were the major carriers for each chemical element. To arrive at the distribution of molecular species, the program considered simultaneously over 370 gaseous and condensed species made up of a minimum of 12 (to a maximum of 16) elements.

It must be pointed out that only those species for which the program was given thermodynamic data were considered in the calculations. Thermodynamic data for some chemically stable condensed phases were not included in the calculations; these phases were solutions, glasses, or slags which might form from the combination of trace metals present in each system. Although some of

these phases would be expected to appear as stable condensed phases, their inclusion at a future time is not expected to significantly perturb the present results with regard to the composition of gaseous carriers or major condensed elements.

The composition results show that, as expected, the major gaseous products for all flames are N_2, O_2, CO_2, H_2O, Ar, NO, OH, CO, and SO_2 with a large number of CHNOS species at lower concentrations. Chlorine appears mainly as HCl. The trace metals exist almost exclusively as either metal oxide or hydroxide molecules. In several of the combustion gas mixtures, condensed phase oxides appear even at the adiabatic flame temperature: e.g., Fe_2O_3 in the light oil, Al_2TiO_5, $CaAl_2Si_2O_8$, $CaTiO_3$, and $CaTiSiO_5$ in the wash solvent, and $Al_6Si_2O_{13}$ and $CaAl_2Si_2O_8$ in the mid:heavy distillate blend.

In order to predict which compounds would condense on the collector surface, the CEC program was run in the T,P mode at 25K temperature intervals from the adiabatic flame temperature down to 1100K. The occurrence of any condensed phases in the calculated compositions was noted. The phases thus identified are listed in Table IX. The phases predicted to condense were given a ranking of strong (s), medium (m), weak (w), very weak (vw), or very, very weak (vvw) to reflect their relative calculated concentrations.

The condensed phases that were indicated by the T,P-mode calculations were divided into three groups: 1) those which appear above 1173K, but which are not present in the results of the calculation at 1173K; 2) those which were the stable phases at 1173K (the target temperature); and 3) those which appear between 1173 and 1100K. The third group was considered because the possible temperature non-uniformity of the collectors (especially the superalloy specimens, which had "cold" ends) might lead to formation of deposits with

dew-points somewhat below 1173K. By scrutinizing Table IX, a prediction of the expected deposit compositions was made. For the naphtha fuel, the deposit is expected to be mainly a mixture of copper and iron oxides, with a small amount of nickel and chromium oxides, possibly some spinels, and a trace of zinc. For the other fuels, the deposit is expected to be mainly Fe_2O_3 in each case, with various smaller amounts of other oxides. Only very low concentrations of sodium sulfate are predicted for the light oil and the only potassium-containing compound appears at low concentration from the wash solvent.

The phases predicted to condense/deposit essentially mirror the presence of the trace metals in each fuel. The only exceptions are: 1) the fairly volatile lead (in the naphtha) and zinc compounds (in the light oil, wash solvent, and mid:heavy blend), which would be predicted to form at temperatures not too far below 1100K; and, 2) potassium (in the light oil), because of its low concentrations and the high stability of KOH(g).

It is significant that either zero or very small amounts of Na_2SO_4 or K_2SO_4 are predicted to form in the deposits. On this basis, and in conjunction with the fact that no significant levels of vanadium were present in the fuels, classical alkali sulfate- or vanadium-induced hot corrosion would not be predicted.

However, due to the presence of metal oxides, fouling of components (that is, build up of deposits) was expected to be a potential problem. A useful extension of the present theoretical analysis would be the calculation of the rates of deposition. Because the severity of fouling is a function of the thickness of deposit, the rate of deposition must be established for each particular situation in order to assess the consequences of this effect. To calculate the amount of deposit as a function of the chemistry, burner and

target geometry, and gas dynamics of the experimental arrangement requires the use of additional sophisticated mass transport theory currently under development with LeRC support (Refs. 24, 25 and 26). Such a treatment is beyond the scope of the present work.

RESULTS AND DISCUSSION

Deposit Analysis and Comparison to Predicted Composition - Measurable amounts of deposits were collected from both the deposition/corrosion and deposition burner rig experiments.

The amounts of deposits collected on the superalloy specimens as a function of time of exposure to the combustion products of SRC-II naphtha are shown in figure 7. The weight change of the samples is taken as a direct measure of the accumulating deposit weight because very little corrosion had occurred. Only very small weight changes are associated with the normal oxidation which the specimens sustained. The two straight lines in figure 7 bracket the range of the weight change data. Typical micrographs of cross-sectioned superalloy specimens after the 191 hour burner rig exposure are shown in figure 8. The porous, friable deposit layers are readily observed. The deposit layers were usually reddish-brown in color. Each photomicrograph also shows a thin layer of oxidized superalloy and an alloy depletion layer. The significance of these will be discussed in the corrosion section below. The average thickness of the deposit layer and the maximum depth of attack of the superalloy are given in Table X. The X-ray diffraction and chemical analysis of the deposits obtained from samples scraped from the superalloy specimens are given in Table XI. The phases identified by X-ray diffraction and the metals detected by the other techniques were given a ranking of strong (s), medium (m), weak (w), or very weak (vw) to reflect

their relative measured concentrations. The deposit phases were identified as mainly CuO(JCPDS card No. 5-661), spinels (a_o=8.38Å) composed of $CuFe_2O_4$(25-283), $(Ni,Zn)Fe_2O_4$(8-234), and $ZnFe_2O_4$(22-1012), $(Cu_{0.2}Ni_{0.8})O$(25-1049), and possibly ZnO(5-664). The chemical techniques identified all of the elements above plus a small amount of chromium. Thus, the agreement between the observed deposit composition (Table XI) and the predicted composition (Table IX) is excellent.

The amounts of the deposits on the Pt-10Rh collectors are listed in Table XII. Micrographs of cross sections of the deposits amd SEM photos of the deposit surface are shown in figure 9. Again, the reddish-brown deposits are seen to be porous and friable. The X-ray diffraction and chemical analysis of the deposits obtained from samples scraped from the collector are given in Table XI. The only phases identified were iron oxides: Fe_2O_3 and Fe_3O_4. A large number of metals in addition to iron were identified by the chemical techniques; all were at low or very low levels. These elements are essentially those detected as the trace metal impurities in the respective fuels and, based on the predictions (Table IX), were expected to form deposits to some degree. Sensitive spot tests for soluble Cl^-, $SO_4^=$, and $S^=$ gave only negative results. The only element that showed up in the chemical analysis, but was not predicted by the thermochemical analysis, was potassium at very low levels from the light oil and blend fuels. The omission of manganese and tin from the calculations apparently did not introduce any serious errors in the prediction of the condensed phase compositions because these elements were not detected in any of the deposits. This is also true for all of the other "minor" trace elements listed in Table I.

Based on the agreement between the predicted and actual compositions of the deposits in all cases, we believe that the procedure employed forms the

basis for a useful and reliable analytical method. This method will permit the prediction of deposit formation in rigs and engines burning coal-derived fuels.

Superalloy Corrosion Tests - As discussed above, the corrosion testing with the naphtha fuel was terminated after 191 cycles (one hour at temperature per cycle) because weight change data (figure 7) indicated very little corrosion had occurred. Had there been rapid corrosion, the overall kinetics would have been such that the weight, which could have initially increased due to the pick up of oxygen (and deposit), would soon peak and then decrease almost linearly. The decrease in weight would be due to the expected spalling of the oxide scale (and any overlaying deposit). In fact, however, the weight of the deposits far exceeded any weight effects due to the corrosion and the data in figure 7 showed weights increasing almost linearly with time. This observation was later confirmed by metallographic examinations (figure 8) which showed a thick deposit and thickness measurements (maximum depth of attack - see Table X) showed the extent of the attack was about the same as that observed for straight oxidation (Ref. 10). The average depth of attack for these alloys in a salt free oxidation test at 1173K is on the order of 50 to 100 μm. Hot corrosion attack would be on the order of hundreds to thousands of micrometers. Thus the Na and K levels in the fuel were too low to permit the significant formation of Na_2SO_4/K_2SO_4 deposits on the specimens which would have initiated accelerated corrosion during the 191 hour exposure experienced here. Instead a benign and porous deposit formed. The chemistry and porosity of this deposit prevented it from having a noticeable effect on the corrosion. Thus the only corrosion was due essentially to oxidation, a slow process for these high temperature alloys at 1173K. These results are in agreement with the thermodynamic calculations which predicted

both the absence of a corrosive deposit of Na_2SO_4/K_2O_4 and the presence of the chemically benign deposit containing mostly copper and iron oxides.

The results obtained here are consistent with those obtained from a DOE-sponsored program at General Electric (Ref. 11). In that program a turbine simulator was used to study hole plugging of film-cooled turbine hot section components. Several fuels were employed: 1) COED (Char-Oil Energy Development), a hydrogenated coal-derived liquid with a C/H ratio of about 1.45; and 2) a synthetic coal-derived liquid fuel consisting of a creasote matrix with various amounts of H-coal sludge. Both deposition and the extent of corrosion were monitored. Although considerable deposition was observed, little or no corrosion took place even though the sodium and potassium levels were at least an order of magnitude higher than in the fuels used in our program.

CONCLUDING REMARKS

The various coal-derived fuels which will be available in the near future should be similar to the fuels tested here. The combustion experience provided by this study has brought to light several potential problem areas in usage of the SRC-II fuels: storage stability; interaction of reactive fuel components with corrosion-susceptible storage and transfer hardware; filter clogging; and, following combustion, fouling by deposits composed of trace metal compounds. Because of the anticipated increased useage of these fuels in the future, problems of deposition, fouling, and possible corrosion should be addressed. Possible control strategies include: 1) fuel pretreatment; 2) fuel additives; 3) altered combustion conditions and gas flows; 4) altered deposition conditions; and 5) development of more corrosion resistant high

temperature alloys and coatings. These recommendations are paralleled by the extensive practical experience gained in the successful use of residual and crude oil fuels in industrial turbines (Refs. 27 and 28).

To implement effectively any of the strategies listed above, an improved understanding of the thermochemistry, kinetics, and dynamics of ash formation, deposition, and corrosion is required. More needs to be done by way of predicting the rates of deposition. Theories of deposition are now being developed to encompass the complete spectrum of particle sizes which may exist from vapors to supermicron size ash or soot particles (Ref. 25). In addition, for a more fundamental understanding, more basic data and theory development are needed in the areas of flame kinetics and mass transport parameters for metal-containing molecules and aerosols.

REFERENCES

1. Liquid Fuels From Coal by the SRC-II Process. Coal Liquefaction Advanced Research Digest, ORNL/FE-2, pp. 1-17, 1979; Schmid, B. K.; and Jackson, D. M.: The SRC-II Process. 2nd Pacific Chemical Engineering Congress, 2nd., Denver, CO, Aug. 27-31, 1977. Vol II. AIChE, 1978, pp. 908-915.
2. Filby, R. H.; Shah, K. R.; and Sautter, C. A.: Trace Elements in the Solvent Refined Coal Process. Symposium Proceedings: Environmental Aspects of Fuel Conversion Technology, 3, EPA-600/7-78-063, pp. 266-282.
3. Stringer, J.: Hot Corrosion of High-Temperature Alloys. Annual Review of Materials Science. Vol. 7. Annual Reviews, Inc., 1977 and references cited therein, p. 477.

4. Smeggil, J. G.; and Bornstein, N. S.: Study of The Effects of Gaseous Environments on the Hot Corrosion of Superalloy Materials. (R79-914387-4, United Technologies Res. Ctr.; NASA Contract NAS3-21376.) NASA CR-159747, 1980.

5. Deadmore, D. L.; and Lowell, C. E.: Airfoil Cooling Hole Plugging by Combustion Gas Impurities of the Type Found in Coal Derived Fuels. DOE/NASA/2593-79/1, NASA TM-79076, 1979.

6. Zellars, G. R.; et al.: The Erosion Corrosion of Small Superalloy Turbine Rotors Operating in the Effluent of a PFB Coal Combustor. NASA TM-79227, 1979; also Advanced Materials for Alternate Fuel Capable Directly Fired Heat Engines. CONF-790749, 1979, pp. 887-912.

7. Clark, J. S.: Status of the DOE/NASA Critical Gas Turbine R&T Project. ASME Paper 80-GT-104, Mar. 1980 and references cited therein.

8. Deadmore D. L.; and Lowell, C. E.: Inhibition of Hot Salt Corrosion by Metallic Additives. DOE/NASA/2593-78/2, NASA TM-78966, 1978.

9. Deadmore, D. L.; and Lowell, C. E.: Effects of Impurities in Coal-Derived Liquids on Accelerated Hot Corrosion of Superalloys. DOE/NASA/2593-79/13, NASA TM-81384, 1980.

10. Lowell, C. E.; Sidik, S. M.; and Deadmore, D. L.: Effect of Sodium, Potassium , Magnesium, Calcium, and Chlorine on the High Temperature Corrosion of IN-100, U-700, IN-792, and Mar M-509. DOE/NASA/2593-79/12, NASA TM-79309, 1980.

11. Sims, C. T.; Doering, H. vonE.; and Smith, D. P.: Effects of the Combustion Products of Coal-Derived Fuels on Gas Turbine Hot-Stage Hardware " ASME Paper 79-GT-160, Mar. 1979; High Temperature Gas Turbine Engine Component Materials Testing Program, Task I, "Fireside I." FE-1765-44, General Electric Company, 1978.

12. Pillsbury, P. W.; et al.: Fuel Effects in Recent Combustion Turbine Burner Tests of Six Coal Liquids. ASME Paper 79-GT-137, Mar. 1979.

13. Callen, R. B.; et al.: Upgrading Coal Liquids to Gas Turbine Fuels. 1. Analytical Characterization of Coal Liquids. Ind. Eng. Chem., Prod. Res. Dev., vol. 15, no. 4, 1976, pp. 222-233.

14. Gordon, W. A.; and Chapman, G. B.: Quantitative Direct-Current Arc Analysis of Random Compositions of Microgram Residues in Silver Chloride Common Matrix. Spectrochim. Acta vol. 25B, 1970, pp. 123-137.

15. Gilbert, P. T., Jr.: Determination of Cadmium by Flame Photometry, Anal. Chem. vol. 31, no. 1, Jan. 1959, pp. 110-114.

16. Lowell, C. E.; and Deadmore, D. L.: Effect of a Chromium-Containing Fuel Additive on Hot Corrosion. Corr. Sci. vol. 18, 1978, pp. 747-763.

17. Santoro, G. J.; Calfo, F. D.; and Kohl, F. J.: Material Response from Mach 0.3 Burner Rig Combustion of a Coal-Oil Mixture. DOE/NASA TM, 1981, in press.

18. Kohl, F. J.; Stearns, C. A.; and Fryburg, G. C.: Sodium Sulfate: Vaporization Thermodynamics and Role in Corrosive Flames. Metal-Slag-Gas Reactions and Processes, Z. A. Foroulis and W. W. Smeltzer, eds., The Electrochemical Society, 1975, pp. 649-664; also NASA TMX-71641, 1975.

19. Kohl, F. J.; et al. Theoretical and Experimental Studies of the Deposition of Na_2SO_4 from Seeded Combustion Gases, J. Electrochem. Soc., vol. 126, no. 6, June 1979, pp. 1054-1061.

20. Miller, R. A.: Analysis of the Response of a Thermal Barrier Coating to Sodium and Vanadium Doped Combustion Gases. DOE/NASA/2593-79/7, NASA TM-79205, 1979.

21. Gordon, S.; and McBride, B. J.: Computer Program for Calculation of Complex Chemical Equilibrium Compositions, Rocket Performance, Incident and Reflected Shocks, and Chapman-Jouget Detonations. NASA SP-273, 1971.

22. Chase, M. W.; et al.: JANAF Thermochemical Tables. Dow Chemical Company, Midland, MI, including supplements to June 1978.

23. Barin, I.; and Knacke, O.: Thermochemical Properties of Inorganic Substances. Springer-Verlag, 1973; Barin, I.; Knacke, O.; and Kubaschewski, O.: Thermochemical Properties of Inorganic Substances, Supplement, Springer-Verlag, 1977.

24. Rosner, D. E.; et al.: Chemically Frozen Multicomponent Boundary Layer Theory of Salt and/or Ash Deposition Rates from Combustion Gases. Combust. Sci. and Technol., vol. 20, 1979, pp. 87-106.

25. Rosner, D. E.; and de La Mora, J. Fernadez: Recent Advances in the Theory of Salt/Ash Deposition in Combustion Systems. Advanced Materials for Alternate Fuel Capable Directly Fired Heat Engines, CONF-790749, pp. 301-330, 1979.

26. Rosner, D. E.; et al.: Transport, Thermodynamic and Kinetic Aspects of Salt/Ash Deposition Rates from Combustion Gases. Proceedings, 10th Materials Research Symposium, Characterization of High Temperature Vapors and Gases. NBS SP-561/2, 1979, pp. 1451-1476.

27. Felix, P. C.: Practical Experience with Crude and Heavy Oil in Stationary Gas Turbines. Brown Boveri Rev., vol. 66, no. 2, Feb. 1979, pp. 89-96.

28. Felix, P. C.: Problems and Operating Experiences with Gas Turbines Burning Residual and Crude Oils. ASME Paper 78-GT-103, Apr. 1978.

TABLE I. - COMPOSITION AND PROPERTIES OF SRC-II FUELS. TRACE ELEMENT ANALYSIS FOR THE NAPHTHA REPORTED IN THIS TABLE WAS FOR A SAMPLE OF FUEL TAKEN AT A POINT IN TIME WHEN THE DEPOSITION/CORROSION TEST HAD BEEN RUN FOR 191 ONE-HOUR CYCLES. TRACE ELEMENT VALUES MARKED WITH AN "*" ARE CONSIDERED IN THE THERMODYNAMIC PREDICTION OF DEPOSITION

	Fuel type			
	Naphtha	Light oil	Wash solvent	Mid:heavy distillate blend
Major elements (weight percent)				
Carbon	84.61 (84.62)[1]	80.45	84.12	86.21
Hydrogen	11.64 (12.09)	9.75	8.80	8.64
Oxygen	3.16 (2.33)	9.17	6.34	3.99
Nitrogen	0.61 (0.58)	0.42	0.53	0.95
Sulfur	0.61 (0.38)	0.40	0.33	0.27
Ash	N.D.[2]	N.D.	N.D.	0.02
Trace elements (wppm)				
Al	<0.01	<0.01	0.9*	1.0*
B	0.08	<0.06	<0.06	<0.09
Ca	<0.01	0.1*	0.6*	0.3*
Cl	49*	<10	<10	294*
Cr	0.1*	0.04	0.06	1.8*
Cu	28.9*	0.03	<<0.01	<0.1
Fe	8.8*	158*	35.7*	7.0*
K	<0.25	0.2*	0.4*	<0.1
Mg	<<0.01	0.08	0.07	0.08
Mn	0.05	0.4	0.3	0.2
Mo	<<0.01	<0.01	<0.01	<<0.01
Na	<0.25	0.6*	0.3*	0.5*
Ni	4.8*	0.1*	<<0.01	0.1*
P	<5	<6	<6	<7
Pb	0.3*	<0.07	<0.06	<0.04
Si	0.09	<0.03	0.5*	1.1*
Sn	0.2	<0.06	<0.06	<0.07
Ti	0.03	<0.01	0.8*	0.2*
V	<<0.01	<0.01	<0.2	0.07
Zn	10.5*	2.5*	0.8*	0.1*
Zr	<<0.01	<0.01	<0.02	<0.02
Chemical composition (vol. %)				
Aromatics	33.0	43.6	62.9	----
Olefins	6.0	----	----	----
Saturates	61.0	----	----	----
Heat of combustion, lower heating value (Btu/lb)	18,497	16,551	16,748	17,590
Sp. Gravity 60/60° F	0.824	----	----	0.999
Viscosity @ 100° F, cSt	0.816	----	----	4.527

[1]Values in parentheses are analysis supplied by P and M upon shipment of SRC-II naphtha.
[2]N.D. = not determined.

TABLE II. - ANALYSIS OF PRECIPITATE FROM SRC-II NAPHTHA FUEL AND THE METAL CONTENT OF THE COKE RECOVERED FROM THE BURNER RIG LINER

Element	Precipitate (weight percent)	Metal content of coke (weight percent)
Al	0.2	0.3
Cr	200 ppm	0.5
Cu	0.2	60
Fe	9.1	16.2
Si	0.2	----
Zn	1.7	20.3
Ni	---	2.3
S	Balance	----

TABLE III. - ANALYSIS OF SRC-II NAPHTHA FUEL FOR TRACE ELEMENTS AND SULFUR AS A FUNCTION OF TIME DURING THE DEPOSITION/CORROSION TEST

Trace element (wppm)	Cycle number		
	0	120	191
Al	0.03	<0.01	<0.01
B	----	----	0.08
Ca	0.04	<0.01	<0.01
Cl	8.5	16	49
Cr	0.1	0.1	0.1
Cu	10	22.1	28.9
Fe	2.4	8.2	8.8
K	<0.25	<0.25	<0.25
Na	0.2	----	<0.25
Ni	0.2	5.2	4.8
Pb	0.3	0.8	0.3
Si	0.06	0.6	0.09
Sn	0.4	0.2	0.2
Ti	0.04	0.04	0.03
Zn	3.0	6.9	10.5
S (weight %)	0.39	0.52	0.61

TABLE IV. - COMPOSITION OF ALLOYS

[All values are weight percent.]

Element	Alloy			
	IN-100	U-700	IN-792	Mar M-509
Cr	10	14.2	12.7	23
Ni	Balance	Balance	Balance	10
Co	15	15.5	9.0	Balance
Al	5.5	4.2	3.2	----
Ti	4.7	3.3	4.2	0.2
Mo	3.0	4.4	2.0	----
W	----	----	3.9	7
Ta	----	----	3.9	3.5
Nb	----	----	0.9	----
V	1.0	----	----	----
Mn	----	<0.01	----	----
Fe	----	0.1	----	----
Si	----	<0.1	----	----
Zr	0.6	<0.01	0.10	0.5
B	0.014	0.02	0.02	----
C	0.18	0.06	0.2	0.6

TABLE V. - INPUT PARAMETERS FOR THE CEC PROGRAM

	SRC-II fuel type			
	Naphtha	Light oil	Wash solvent	Mid:heavy distillate blend
Fuel composition a) Stoichiometry of carbon, hydrogen, nitrogen, and oxygen	$C_{1.00}$ $H_{1.6397}$ $N_{0.0062}$ $O_{0.0280}$	$C_{1.00}$ $H_{1.4441}$ $N_{0.0045}$ $O_{0.0856}$	$C_{1.00}$ $H_{1.3810}$ $N_{0.0054}$ $O_{0.0818}$	$C_{1.00}$ $H_{1.1945}$ $N_{0.0094}$ $O_{0.0348}$
b) Sulfur, weight fraction of fuel	0.0061	0.0040	0.0033	0.0027
c) Trace elements, weight fraction of fuel				
Al	---	---	9.0×10^{-7}	1.0×10^{-6}
Ca	---	1.0×10^{-7}	6.0×10^{-7}	3.0×10^{-7}
Cl	4.9×10^{-5}	---	---	2.94×10^{-4}
Cr	1.0×10^{-7}	---	---	1.8×10^{-6}
Cu	2.89×10^{-5}	---	---	---
Fe	8.8×10^{-6}	1.58×10^{-4}	3.57×10^{-5}	7.0×10^{-6}
K	---	2.0×10^{-7}	4.0×10^{-7}	---
Na	---	6.0×10^{-7}	3.0×10^{-7}	5.0×10^{-7}
Ni	4.8×10^{-6}	1.0×10^{-7}	---	1.0×10^{-7}
Pb	3.0×10^{-7}	---	---	---
Si	---	---	5.0×10^{-7}	1.1×10^{-6}
Ti	---	---	8.0×10^{-7}	2.0×10^{-7}
Zn	1.05×10^{-5}	2.5×10^{-6}	8.0×10^{-7}	1.0×10^{-7}
Assigned enthalpy of fuel (cal mol^{-1}) at inlet temperature of 298 K	-930	-11 880	-9170	651
Composition of air	$N_{1.56176}O_{0.41959}Ar_{0.009324}C_{0.000300}$			
Moisture in air, (wt. %)[1]	1.0	1.0	1.0	1.0
Assigned enthalpy of air (cal mol^{-1}) at inlet temperature (in parentheses)	2639 (672 K)	2433 (644 K)	2433 (644 K)	2433 (644 K)
Pressure, (atm)	1.0	1.0	1.0	1.0
Fuel-to-air mass ratio	0.0400	0.0350	0.0398	0.0450

[1]Approximately 50 percent relative humidity at 298 K.

TABLE VI. - GASEOUS ELEMENTS AND COMPOUNDS CONSIDERED IN THE CEC PROGRAM

Common gaseous combustion products (for fuel-lean flames):
N_2, O_2, CO_2, H_2O, CO, NO, NO_2, N_2O, OH, O, H, H_2, SO, SO_2,

SO_3, H_2SO_4, H_2S, Cl, HCl, Ar plus many trace species

containing the elements C, H, O, N, S, and/or Cl

Alkali- and alkaline-earth-containing gases:
Ca, CaCl, $CaCl_2$, CaO, CaOH, $Ca(OH)_2$

K, KH, KO, KOH, $(KOH)_2$, K_2SO_4

Na, NaCl, $(NaCl)_2$, NaH, NaO, NaOH, Na_2O, $(NaOH)_2$, Na_2SO_4

Metal-containing gases:
Al, AlCl, $AlCl_2$, $AlCl_3$, Al_2Cl_6, AlOCl, AlH, AlN, AlO, AlS, AlOH, AlO_2, AlO_2H, Al_2O, Al_2O_2

Cr, CrN, CrO, CrO_2, CrO_3, CrO_2Cl_2

Cu, CuCl, Cu_3Cl_3, CuO, Cu_2

Fe, FeCl, $FeCl_2$, $FeCl_3$, Fe_2Cl_4, Fe_2Cl_6, FeO, $Fe(OH)_2$, FeS

Ni, NiCl, $NiCl_2$, NiO, $Ni(OH)_2$, NiS

Pb, PbCl, $PbCl_2$, $PbCl_4$, PbO, PbS, Pb_2

Si, SiCl, $SiCl_2$, $SiCl_3$, $SiCl_4$, SiN, SiO, SiO_2, SiS, Si_2

Ti, TiCl, $TiCl_2$, $TiCl_3$, $TiCl_4$, TiO, TiOCl, $TiOCl_2$, TiO_2

Zn, ZnO

Plus other minor metal-containing species not listed

TABLE VII. - CONDENSED METAL-CONTAINING PHASES CONSIDERED IN THE CEC PROGRAM

Metal	Condensed phases
Al	$AlCl_3$, AlN, Al_2O_3, Al_2S_3, $Al_2(SO_4)_3$
Ca	$CaCl_2$, $CaCO_3$, CaO, $Ca(OH)_2$, CaS, $CaSO_3$, $CaSO_4$
Cr	CrN, Cr_2N, Cr_2O_3, CrS, $Cr_2(SO_4)_3$
Cu	$CuCO_3$, CuO, Cu_2O, $Cu(OH)_2$, CuS, Cu_2S, $CuSO_4$, Cu_2OSO_4
Fe	$FeCl_2$, $FeCl_3$, FeO, FeOCl, Fe_2O_3, Fe_3O_4, $Fe(OH)_2$, $Fe(OH)_3$, FeS, FeS_2, $FeSO_4$, $Fe_2(SO_4)_3$
K	KCN, K_2CO_3, KO_2, K_2O, K_2O_2, KOH, K_2S, K_2SO_3, K_2SO_4
Na	NaCl, NaCN, Na_2CO_3, NaO_2, Na_2O, Na_2O_2, NaOH, Na_2S, Na_2SO_3, Na_2SO_4
Ni	NiO, NiS, NiS_2, Ni_3S_2, Ni_3S_4, $NiSO_4$
Pb	$PbCl_2$, PbO, PbO_2, Pb_3O_4, PbS, $PbSO_4$
Si	SiO_2
Ti	TiC, $TiCl_2$, $TiCl_3$, $TiCl_4$, TiN, TiO, TiO_2, Ti_2O_3, Ti_3O_5, Ti_4O_7
Zn	ZnO, $Zn(OH)_2$, ZnS, $ZnSO_4$
	Mixed metal phases
	Al_2SiO_5, $Al_2Si_2O_7$, Al_2TiO_5, $Al_6Si_2O_{13}$,
	$CaAl_2O_4$, $CaAl_2SiO_6$, $CaAl_2Si_2O_8$, $CaAl_4O_7$, $CaFe_2O_4$,
	$CaSiO_3$, $CaTiO_3$, $CaTiSiO_5$, $Ca_2Al_2SiO_7$, $Ca_2Fe_2O_5$,
	Ca_2SiO_4, $Ca_3Al_2O_6$, $Ca_3Al_2Si_3O_{12}$, Ca_3SiO_5, $Ca_3Si_2O_7$,
	$Ca_3Ti_2O_7$, $Ca_4Ti_3O_{10}$
	$CuFe_2O_4$, $Cu_2Fe_2O_4$
	$FeAl_2O_4$, $FeTiO_3$, Fe_2SiO_4
	$KAlSi_3O_8$, $K_2Al_2Si_2O_8$, K_2SiO_3, $K_2Si_4O_9$
	$NaAlO_2$, Na_2CrO_4, $Na_2Al_2Si_4O_{12}$, $Na_2Al_2Si_6O_{16}$, $Na_2Fe_2O_4$,
	Na_2SiO_3, $Na_2Si_2O_5$, Na_2TiO_3, Na_4SiO_4, $Na_6Si_2O_7$
	$NiAl_2O_4$, $NiCr_2O_4$, $NiFe_2O_4$

TABLE VIII. - ADIABATIC FLAME TEMPERATURES AND COMPOSITION OF COMBUSTION PRODUCTS FROM SCR-II FUELS CONTAINING TRACE METAL IMPURITIES

		Fuel type			
		Naphtha	Light oil	Wash solvent	Mid:heavy distillate blend
Calculated adiabatic flame temperature, K		1894	1587	1713	1940
Composition of combustion products, major species (mole fraction)	N_2	7.4×10^{-1}	7.5×10^{-1}	7.5×10^{-1}	7.4×10^{-1}
	CO_2	7.8×10^{-2}	6.6×10^{-2}	7.5×10^{-2}	9.0×10^{-2}
	CO	1.3×10^{-4}	3.3×10^{-6}	1.9×10^{-5}	2.4×10^{-4}
	H_2O	7.9×10^{-2}	6.3×10^{-2}	6.7×10^{-2}	6.9×10^{-2}
	O_2	8.8×10^{-2}	1.1×10^{-1}	1.0×10^{-1}	8.2×10^{-2}
	Ar	8.9×10^{-3}	8.9×10^{-3}	8.9×10^{-3}	8.9×10^{-3}
	NO	3.8×10^{-3}	1.4×10^{-3}	2.2×10^{-3}	4.2×10^{-3}
	OH	8.6×10^{-4}	1.1×10^{-4}	2.8×10^{-4}	1.0×10^{-3}
	SO_2	2.1×10^{-4}	1.2×10^{-4}	1.1×10^{-4}	1.1×10^{-4}
Trace element species	AlO_2H	---	---	4.1×10^{-10}	3.0×10^{-8}
	AlO_2	---	---	2.0×10^{-12}	4.9×10^{-10}
	$Al_6Si_2O_{13}(S)$	---	---	---	1.7×10^{-9}
	$Al_2TiO_5(S)$	---	---	1.1×10^{-8}	---
	$Ca(OH)_2$	---	2.4×10^{-9}	1.8×10^{-9}	6.5×10^{-9}
	CaOH	---	1.3×10^{-13}	4.8×10^{-13}	1.8×10^{-11}
	$CaAl_2Si_2O_8(\ell)$	---	---	7.4×10^{-9}	2.9×10^{-9}
	$CaTiO_3(S)$	---	---	2.6×10^{-9}	---
	$CaTiSiO_5(\ell)$	---	---	4.8×10^{-9}	---
	HCl	7.0×10^{-7}	---	---	4.6×10^{-6}
	Cl	6.9×10^{-8}	---	---	5.6×10^{-7}
	CrO_3	1.3×10^{-9}	---	---	2.2×10^{-8}
	CrO_2	8.9×10^{-10}	---	---	2.2×10^{-8}
	Cu	4.9×10^{-7}	---	---	---
	CuO	1.7×10^{-8}	---	---	---
	$Fe(OH)_2$	1.7×10^{-7}	1.9×10^{-7}	7.1×10^{-7}	1.5×10^{-7}
	FeO	6.5×10^{-9}	2.0×10^{-10}	4.0×10^{-9}	1.0×10^{-8}
	$Fe_2O_3(S)$	---	1.3×10^{-6}	---	---
	KOH	---	5.0×10^{-9}	1.1×10^{-8}	---
	K	---	2.1×10^{-11}	1.4×10^{-10}	---
	NaOH	---	2.5×10^{-8}	1.4×10^{-8}	2.0×10^{-8}
	Na	---	4.4×10^{-10}	6.4×10^{-10}	4.2×10^{-9}
	$Ni(OH)_2$	7.2×10^{-8}	1.7×10^{-9}	---	1.4×10^{-9}
	NiO	1.4×10^{-8}	8.6×10^{-12}	---	5.0×10^{-10}
	PbO	1.4×10^{-9}	---	---	---
	Pb	1.9×10^{-10}	---	---	---
	SiO_2	---	---	2.4×10^{-10}	3.3×10^{-8}
	SiO	---	---	8.2×10^{-12}	6.5×10^{-9}
	TiO_2	---	---	2.0×10^{-10}	5.3×10^{-9}
	TiO	---	---	6.5×10^{-17}	3.6×10^{-14}
	ZnO	1.7×10^{-7}	3.7×10^{-8}	1.3×10^{-8}	1.8×10^{-9}
	Zn	9.5×10^{-9}	3.2×10^{-10}	2.7×10^{-10}	1.3×10^{-10}

TABLE IX. - COMPUTER PROGRAM ANALYSIS OF CONDENSED PHASE COMPOSITIONS OF DEPOSITS FROM SRC-II LIQUID FUELS

	Fuel type			
	Naphtha	Light oil	Wash solvent	Mid:heavy distillate blend
Condensed phases which appear above 1173 K, but which are not present at 1173 K	Cu_2O(s)[1] Fe_2O_3(m) $CuFe_2O_4$(w) $Cu_2Fe_2O_4$(w) Cr_2O_3(vw)	$CaFe_2O_4$(vw)	Al_2TiO_5(w) $CaAl_2Si_2O_8$(vw) $CaTiO_3$(vw)	$Al_6Si_2O_{13}$(w)
Condensed phases at 1173 K	CuO(s) $NiFe_2O_4$(m) $NiCr_2O_4$(w)	Fe_2O_3(s) $CaSO_4$(vw) $NiFe_2O_4$(vw)	Fe_2O_3(s) $Al_2Si_2O_7$(w) $CaTiSiO_5$(w) $KAlSi_3O_8$(w) $Na_2Al_2Si_6O_{16}$(vw)	Fe_2O_3(s) Cr_2O_3(m) Al_2SiO_5(w) Al_2TiO_5(w) $CaAl_2Si_2O_8$(w) SiO_2(w) $Na_2Al_2Si_6O_{16}$(vw) $NiFe_2O_4$(vw)
Condensed phases which appear between 1173 and 1100 K	ZnO(w) NiO(vw)	Na_2SO_4(vvw)	---	---

[1]s = strong; m = medium; w = weak; vw = very weak; vvw = very, very weak.

TABLE X. - THICKNESS OF DEPOSIT AND MAXIMUM DEPTH OF ATTACK AFTER 191 HOUR BURNER RIG EXPOSURE TO THE COMBUSTION PRODUCTS FROM SRC-II NAPHTHA

Sample number	Alloy	Average thickness of deposit, μm	Maximum depth of attack, μm
1	IN-100	100	68
2	U-700	116	17
3	U-700	71	43
4	IN-792	98	51
5	IN-792	100	26
6	Mar M-509	70	34
7	Mar M-509	47	58

TABLE XI. - DEPOSIT ANALYSIS

Technique	Fuel type			
	Naphtha	Light oil	Wash solvent	Mid:heavy distillate blend
X-ray diffraction	$CuO(s)$[1] $(Cu,Ni,Zn)Fe_2O_4(s)$ $(Cu_{0.2}Ni_{0.8})O(m)$ $ZnO(vw)$	$Fe_2O_3(s)$	$Fe_2O_3(s)$ $Fe_3O_4(s)$	$Fe_2O_3(s)$
Emission spectroscopy, metallic elements	Cu(s) Fe(m) Ni(m) Zn(m) Cr(w)	Fe(s) Si(w) Al(w) Zn(w) Cu(vw) Ni(vw) Ti(vw) Cr(vw)	Fe(s) Si(m) Al(m) Cu(m) Ni(w) Zn(w) Ti(w) Ca(vw) Cr(vw)	Fe(s) Si(m) Al(w) Ca(w) Ti(w) Cr(vw)
X-ray spectral analysis, metallic elements	Cu(s) Fe(s) Ni(s) Zn(s)	Fe(s) Cu(vw) K (vw) Ca(vw)	Fe(s) Si(m) Al(m) Cu(vw) K (vw) Ca(vw) Ti(vw)	Fe(s) Si(s) Al(m) Ca(m) Ti(w) K (w) Zn(w)

[1]s = strong; m = medium; w = weak; vw = very weak.

TABLE XII. - AMOUNT OF DEPOSIT COLLECTED ON THE 5.07 cm^2 Pt-10Rh COLLECTOR AT 1173 K (mg h^{-1})

Run number	Fuel type		
	Light oil	Wash solvent	Mid:heavy distillate blend
1	9.5	14.3	22.5
2	14.8	16.3	4.2

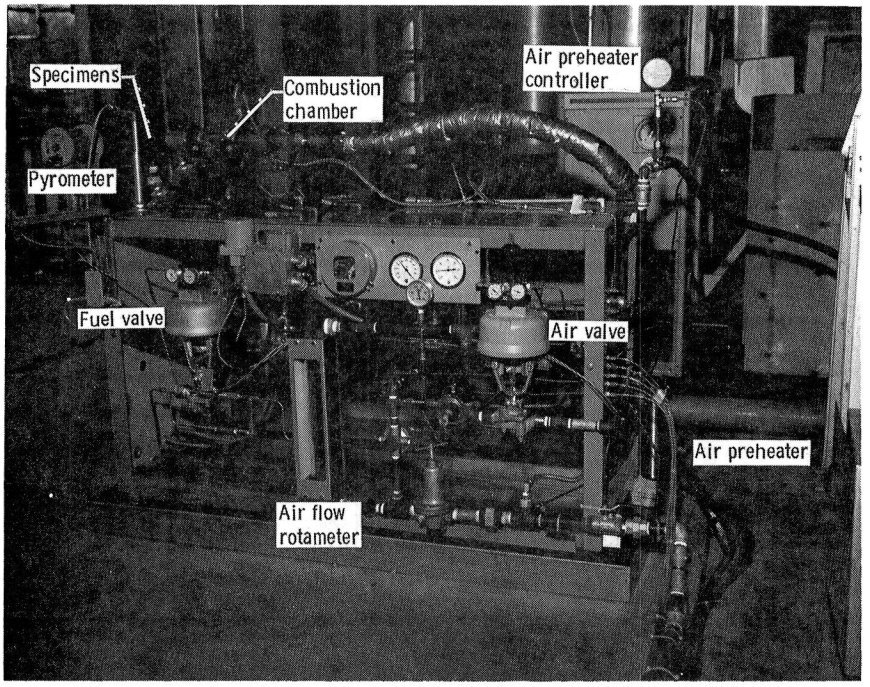

(a) Photograph of rig on stand

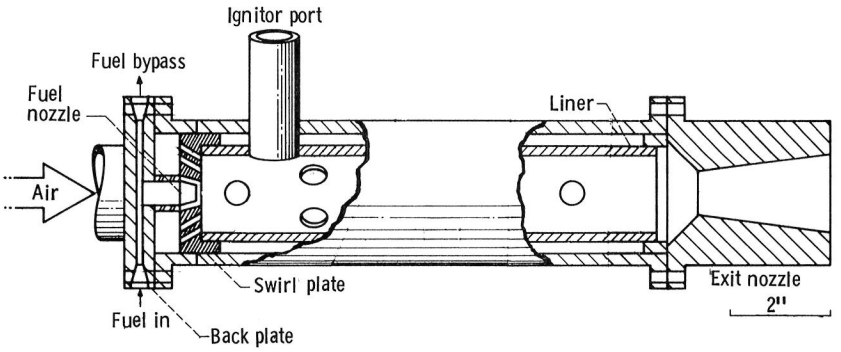

Burner housing and liner with swirl plate

(b) Schematic cross-section combustion chamber

Figure 1. - Mach 0.3 burner rig.

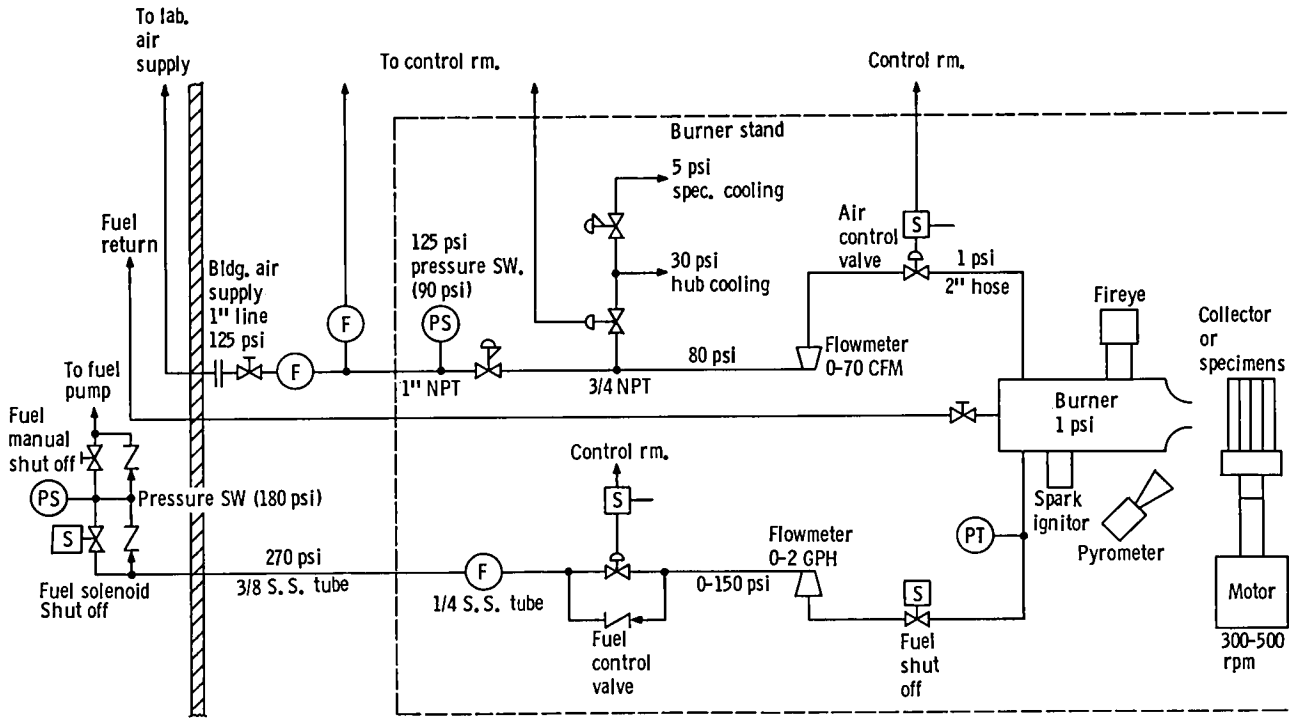

Figure 2. - Air and fuel supply schematic for Mach 0.3 burner rig.

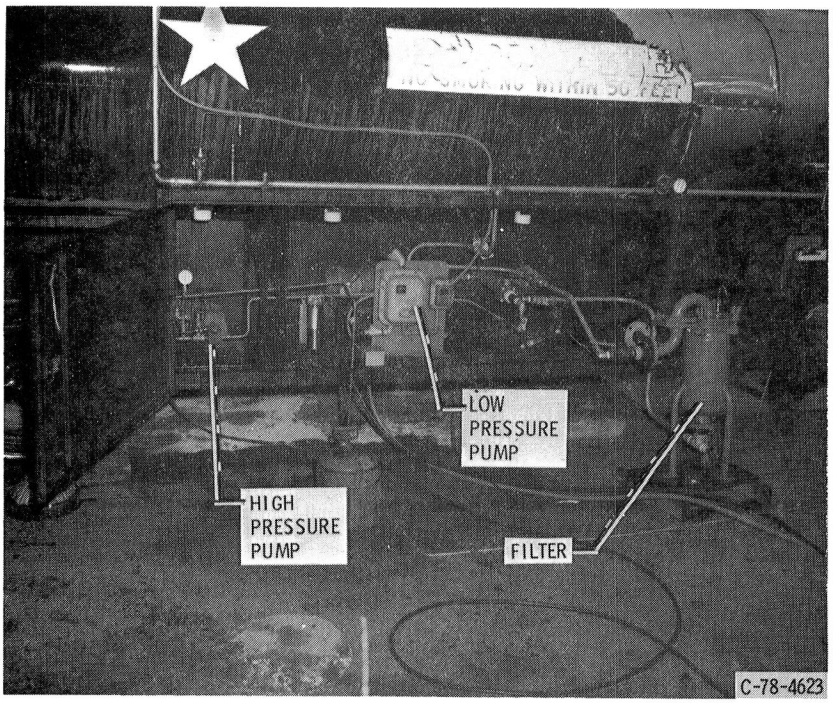

(a) FUEL PUMPS AND HARDWARE FOR DELIVERY OF SRC-11 NAPHTHA FUEL

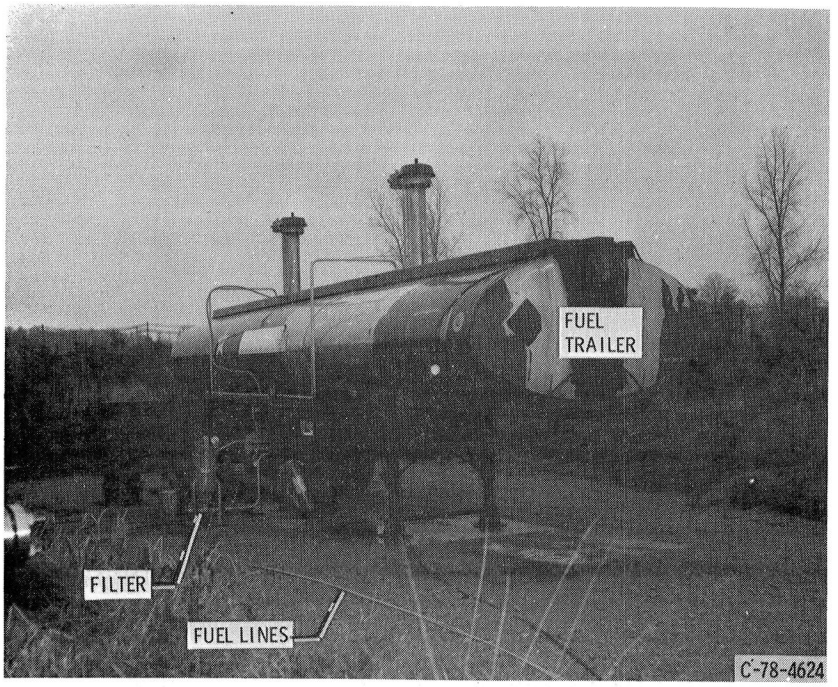

(b) FUEL TRAILER AND STORAGE SITE

Figure 3. - Burner rig fuel supply.

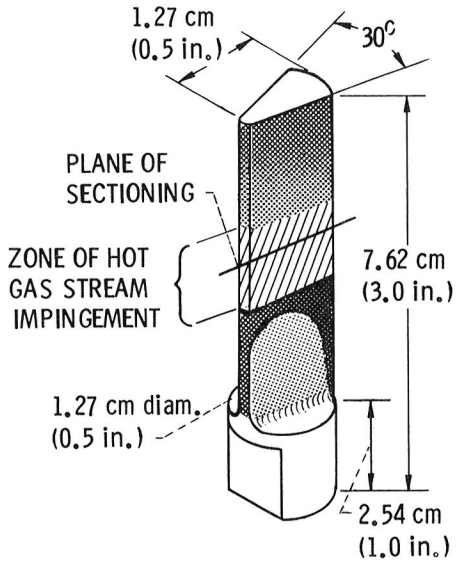

Figure 4. - Deposition/corrosion test specimen.

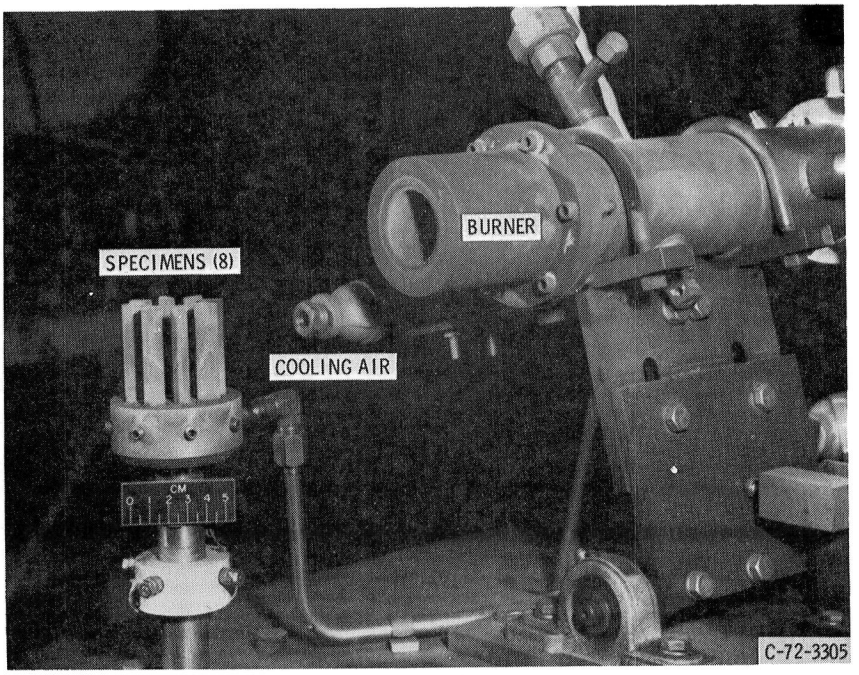

Figure 5. - Burner rig and superalloy test specimens.

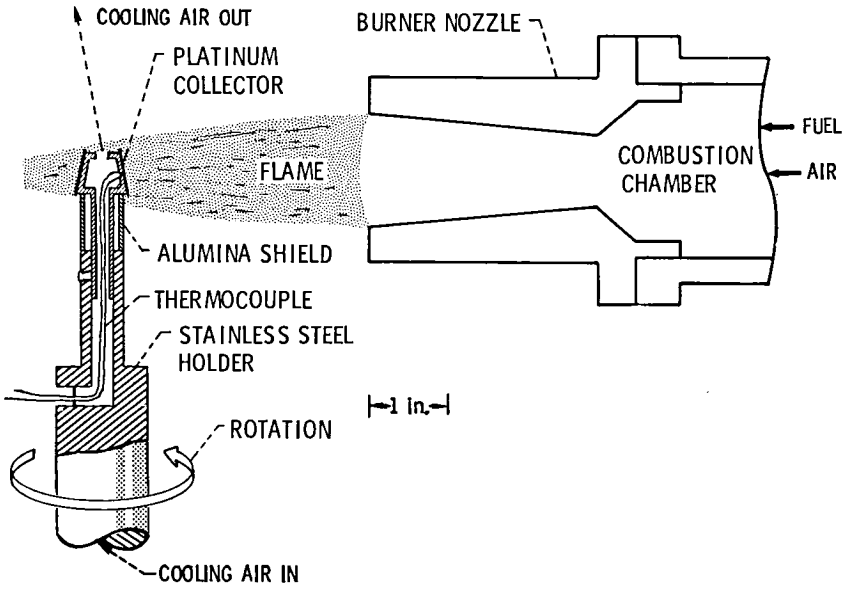

Figure 6. - Schematic cross-section of burner rig deposition apparatus.

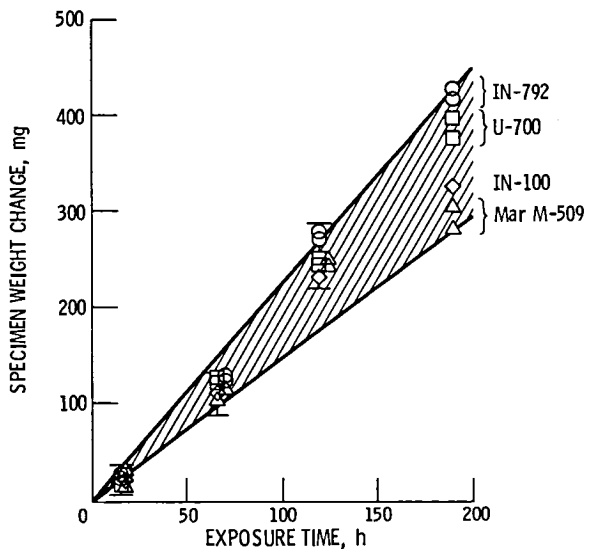

Figure 7. - Superalloy specimen weight change as a function of exposure time to combustion products of SRC-II naphtha. The two straight lines bracket the range of the data.

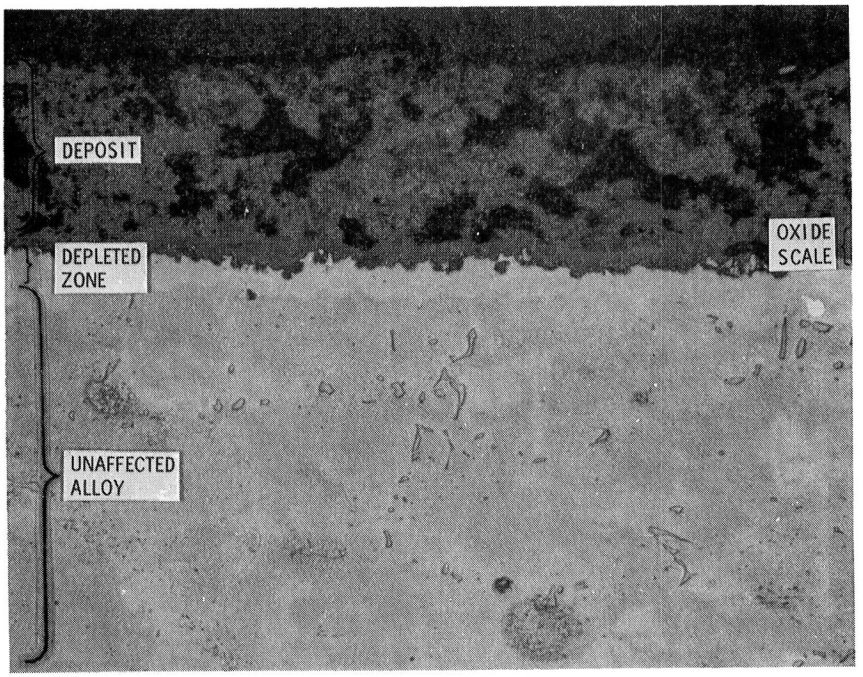

(a) IN-100

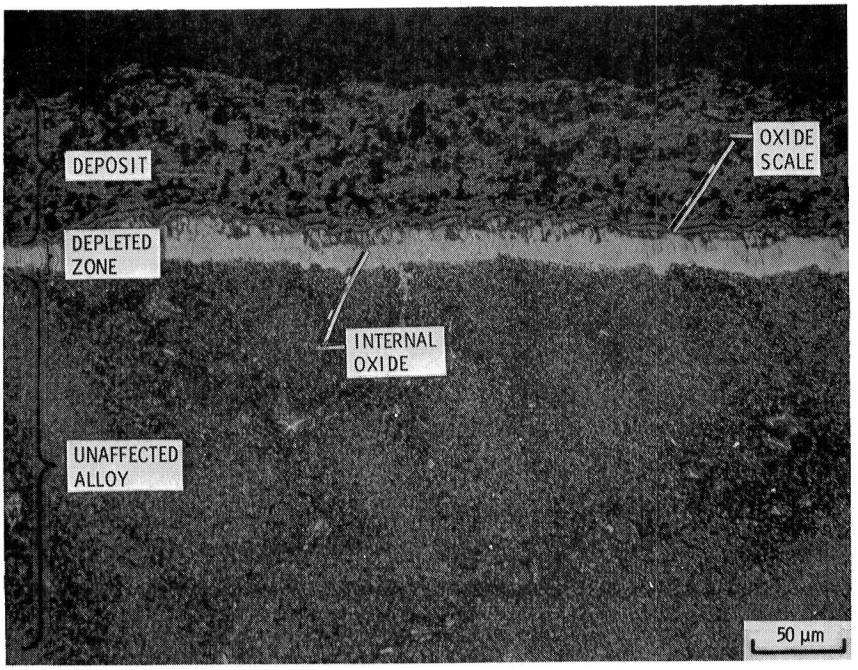

(b) U-700

Figure 8. - Typical micrographs of cross-sectioned superalloy specimens after 191 hours of burner rig exposure of 900° C with SRC-11 naphtha fuel.

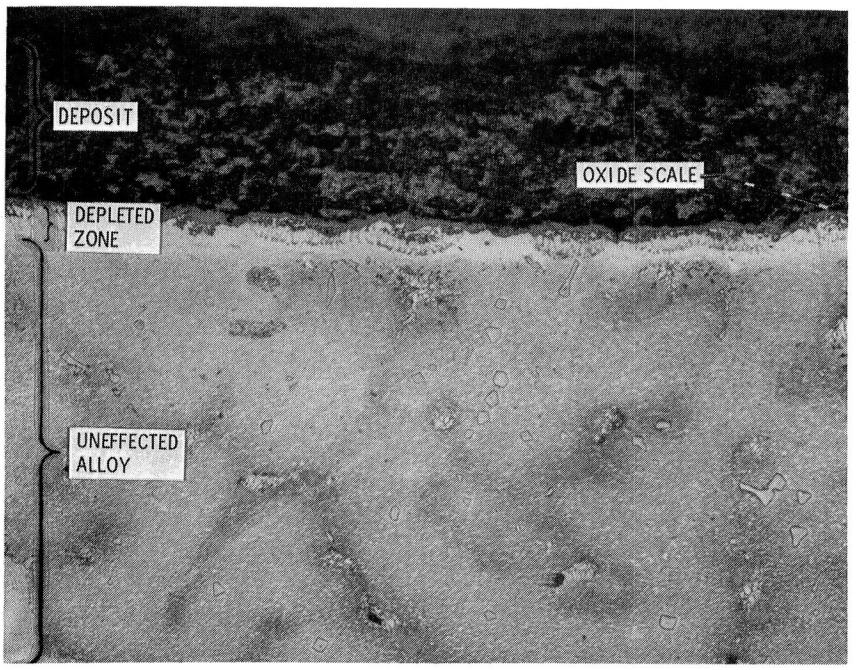

(c) IN-792

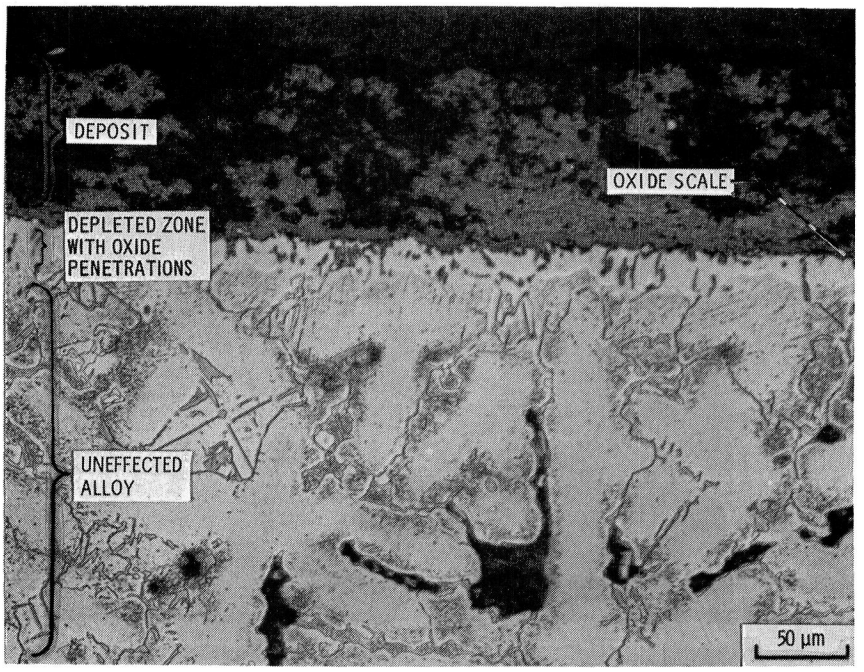

(d) Mar M-509

Figure 8. - Concluded.

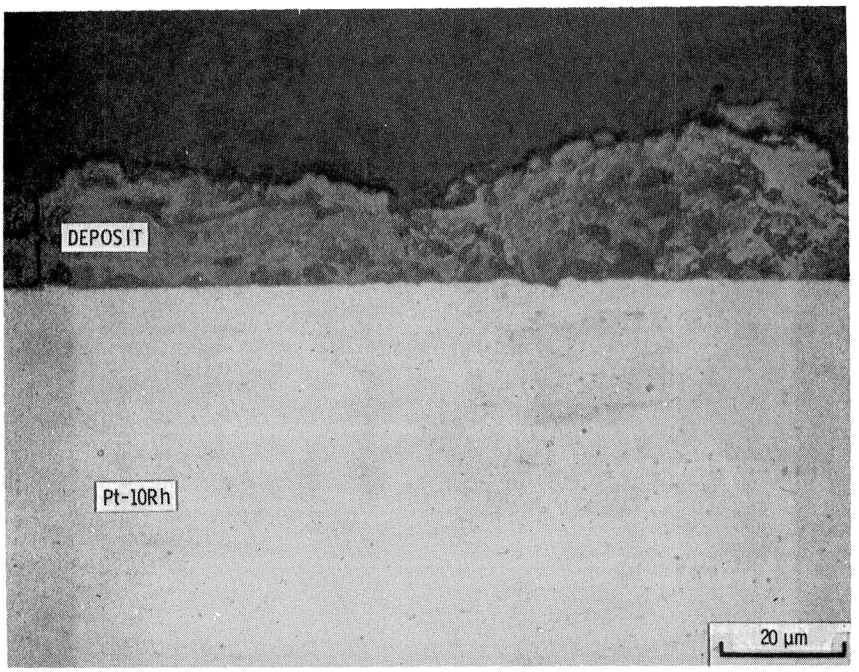

(a) CROSS SECTION

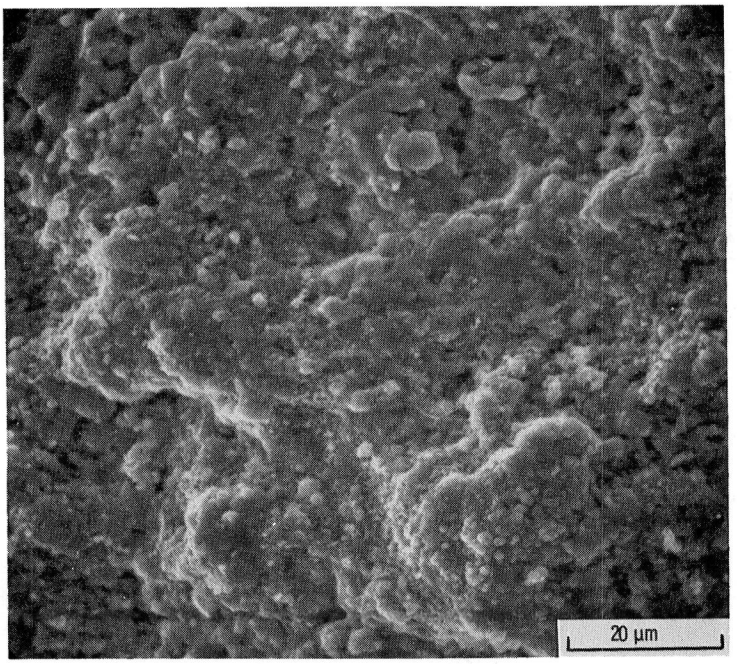

(b) SURFACE

FUEL: LIGHT OIL

Figure 9. - Micrographs of deposits from SRC-II light oil, wash solvent, and blend fuels on Pt-10Rh collector.

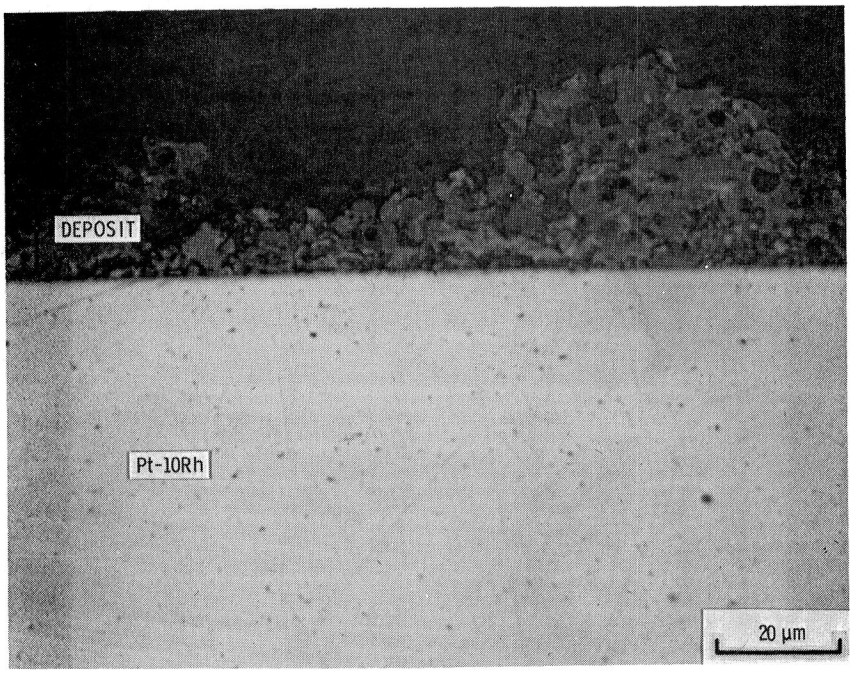

(c) CROSS SECTION

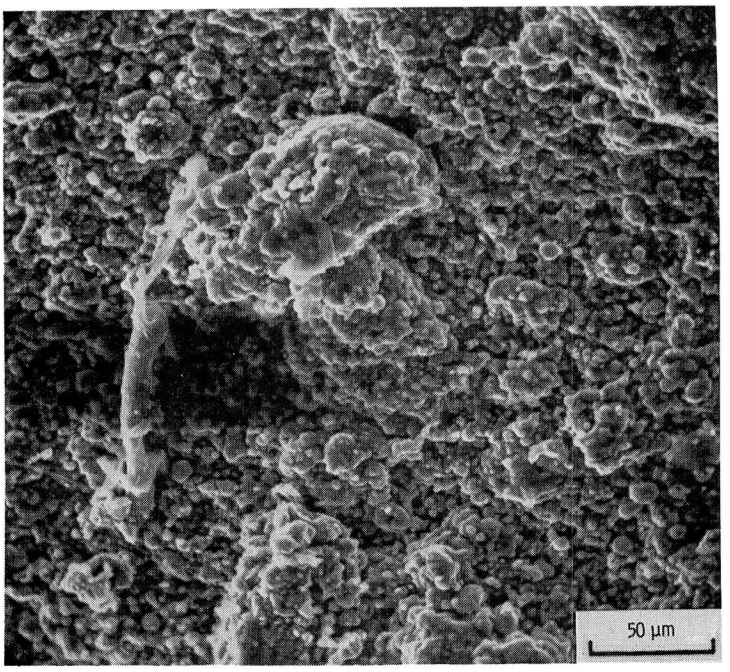

(d) SURFACE

FUEL: WASH SOLVENT

Figure 9. - Continued.

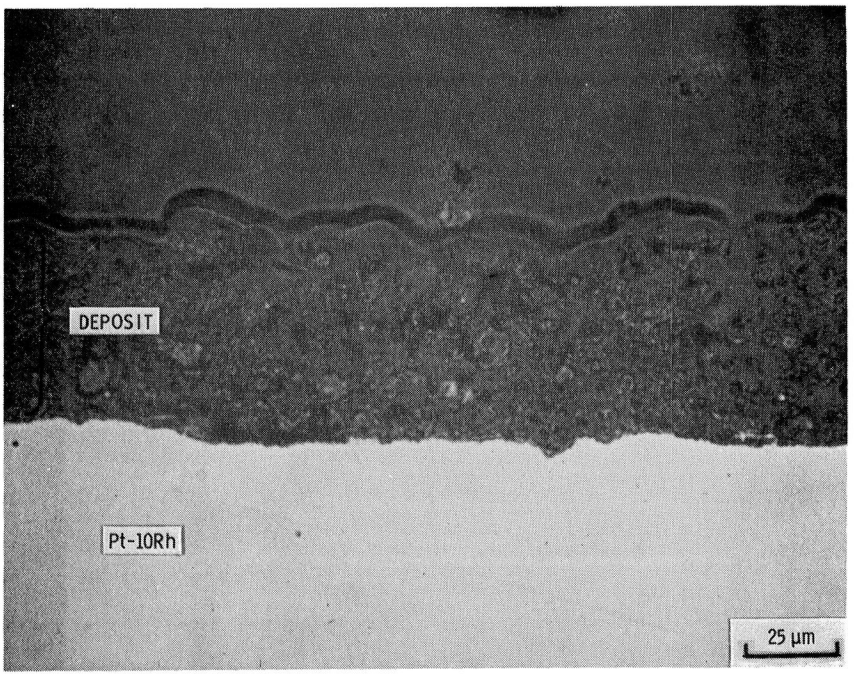

(e) CROSS SECTION

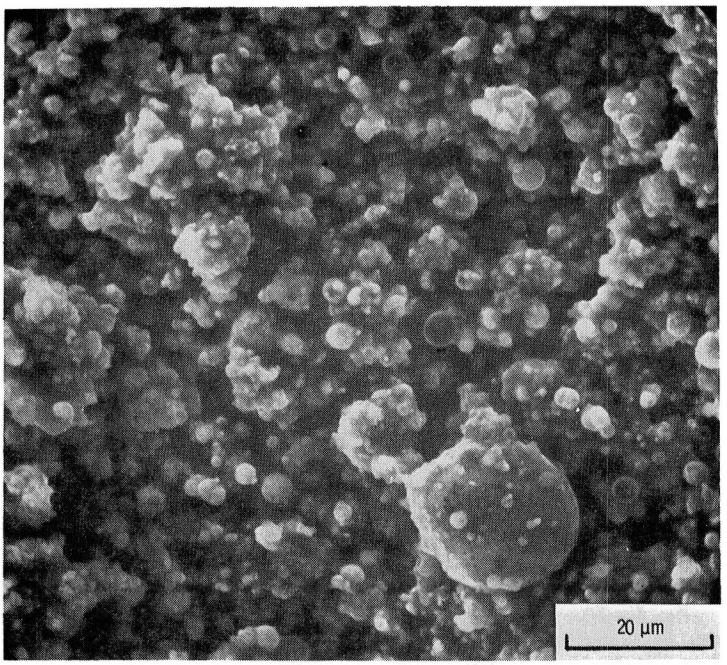

(f) SURFACE

FUEL: MID:HEAVY DISTILLATE BLEND

Figure 9. - Concluded.

1. Report No. NASA TM-81634	2. Government Accession No.	3. Recipient's Catalog No.
4. Title and Subtitle DEPOSITION AND MATERIAL RESPONSE FROM MACH 0.3 BURNER RIG COMBUSTION OF SRC-II FUELS		5. Report Date October 1980 6. Performing Organization Code 778-11-06
7. Author(s) G. J. Santoro, F. J. Kohl, C. A. Stearns, G. C. Fryburg, and J. R. Johnston		8. Performing Organization Report No. E-647 10. Work Unit No.
9. Performing Organization Name and Address National Aeronautics and Space Administration Lewis Research Center Cleveland, Ohio 44135		11. Contract or Grant No. 13. Type of Report and Period Covered Technical Memorandum
12. Sponsoring Agency Name and Address U.S. Department of Energy Office of Coal Utilization Washington, D.C. 20545		14. Sponsoring Agency Code Report No. DOE/NASA/2593-20

15. Supplementary Notes

Final report. Prepared under Interagency Agreement EF-77-A-01-2593.

16. Abstract

Collectors at 1173K (900°C) were exposed to the combustion products of a Mach 0.3 burner rig fueled with various SRC-II fuels (i.e., industrial turbine liquid fuels from solvent refined coals). Four fuels were employed - a naphtha, a lignt oil, a wash solvent and a mid:heavy distillate blend. The response of four superalloys (IN-100, U-700, IN-792 and MarM-509) to exposure to the combustion gases from the SRC-II naphtha and resultant deposits was also determined. The SRC-II fuel analysis and insights obtained during the combustion experience are discussed. Particular problems encountered were fuel instability and reactions of the fuel with hardware components. The major metallic elements which contributed to the deposits were copper, iron, chromium, calcium, aluminum, nickel, silicon, titanium, zinc, and sodium. The deposits were found to be mainly metal oxides. An equilibrium thermodynamic analysis was employed to predict the chemical composition of the deposits. The agreement between the predicted and observed compounds was excellent. No hot corrosion was observed. This was expected because the deposits contained very little sodium or potassium and consisted mainly of the unreactive oxides. However, the amounts of deposits formed indicated that fouling is a potential problem with the use of these fuels.

17. Key Words (Suggested by Author(s))	18. Distribution Statement
Coal-derived fuel; Hot corrosion; Chemical equilibrium; Computer program; Deposition; Combustion products; Fuel combustion; Fuel impurities; Superalloy; Fouling	Unclassified - unlimited STAR Category 26 DOE Category UC-90h

19. Security Classif. (of this report)	20. Security Classif. (of this page)	21. No. of Pages	22. Price*
Unclassified	Unclassified		

* For sale by the National Technical Information Service, Springfield, Virginia 22161